

BATCH IMPLICIT NEURAL REPRESENTATION FOR MRI PARALLEL RECONSTRUCTION

Hao Li^{1,†}, Yusheng Zhou^{2,†}, Jianan Liu^{3,*}, Xiling Liu⁴, Tao Huang⁵, and Zhihan Lv⁶

¹ The Department of Neuroradiology, University Hospital Heidelberg, Heidelberg, Germany;

² School of Electrical Engineering and Automation, Wuhan University, Wuhan, China;

³ Vitalent Consulting, Gothenburg, Sweden;

⁴ Department of Stomatology, Shenzhen People’s Hospital, Shenzhen, China;

⁵ The College of Science and Engineering, James Cook University, Cairns, Australia;

⁶ Department of Game Design, Faculty of Arts, Uppsala University, Sweden.

ABSTRACT

Magnetic resonance imaging (MRI) always suffered from the problem of long acquisition time. MRI reconstruction is one solution to reduce scan time by skipping certain phase-encoding lines and then restoring high-quality images from undersampled measurements. Recently, implicit neural representation (INR) has emerged as a new deep learning method that represents an object as a continuous function of spatial coordinates, and this function is normally parameterized by a multilayer perceptron (MLP). In this paper, we propose a novel MRI reconstruction method based on INR, which represents the fully-sampled images as the function of pixel coordinates and prior feature vectors of undersampled images for overcoming the generalization problem of INR. Specifically, we introduce a scale-embedded encoder to produce scale-independent pixel-specific features from MR images with different undersampled scales and then concatenate with coordinates vectors to recover fully-sampled MR images via an MLP, thus achieving arbitrary scale reconstruction. The performance of the proposed method was assessed by experimenting on publicly available MRI datasets and compared with other reconstruction methods. Our quantitative evaluation demonstrates the superiority of the proposed method over alternative reconstruction methods.

Index Terms—

Magnetic resonance imaging, parallel imaging reconstruction, implicit neural representation, supervised learning

1. INTRODUCTION

Magnetic Resonance Imaging (MRI) stands as a pivotal non-ionizing medical imaging modality. A persistent concern in MRI is the protracted acquisition duration. Strategies to enhance MRI acquisition speed while preserving image fidelity entail omitting phase-encoding lines in K-space, followed by

image reconstruction from the undersampled data. Noteworthy methodologies include compressed sensing (CS) [1] and parallel imaging (PI) [2, 3]. CS leverages signal sparsity to form an observation matrix, thereby reconstructing artifact-free images from randomly undersampled K-space. PI leverages the redundancy inherent in multiple receiving coil elements to abbreviate phase encoding steps periodically. Nevertheless, both CS and PI are susceptible to noise and aliasing artifacts at high undersampling factors.

Recently, deep learning-based methods have shown great potential in MRI reconstruction tasks. These methods can be divided into two types: data-driven and model-driven [4]. The data-driven methods [5, 6] train end-to-end neural networks for learning the potential mapping from undersampled MR images to fully-sampled MR images. In contrast, the model-driven methods [7, 8] unroll the conventional reconstruction iterative algorithm and use networks to learn the auxiliary parameters or regularizations. All these methods have demonstrated significant improvements over both conventional CS-based and PI-based methods and achieved impressive performance. However, most of the existing deep learning-based methods are designed to reconstruct MRI with a fixed undersampled scale and must be trained and stored for each scale factor respectively, which is very computationally expensive and resource-intensive.

Over the past years, implicit neural representation (INR) has emerged with rising popularity in various tasks in computer vision. It is designed to model the 2D slice or 3D volume as a continuous function of spatial coordinates and parameterize the function [9]. A well-known INR-based work proposed by Mildenhall *et al.* [10] is the neural radiance fields (NeRF), which represented a scene by a fully connected deep network to render novel views with impressive visual quality. Besides, INR has also been applied to medical image tasks. An INR-based super-resolution method was proposed to upsample the MRI volume at arbitrary scales in a continuous domain [11, 12]. NeRP [13] reconstructed static MRI from the sparsely sampled k-space data with prior embedding.

[†] Authors contribute equally to the work and are co-first authors.

* Corresponding Author, Email: jianan.liu@vitalent.se

NeSVoR [14] reconstructed MR volume from slice based on INR. All of this work has yielded interesting results. However, the main drawback is to train a specific network for each image slice, resulting in hours for each subject [15], which is time-consuming and impractical in real clinics.

Inspired by these INR-based works, we applied INR to the reconstruction of the parallel imaging of MRI. Specifically, we propose a method that learns a continuous implicit neural voxel function to represent fully sampled MR images and extend the implicit function to overcome the scale-specific constraint of existing deep learning-based reconstruction methods and the subject-specific constraint of INR. This function takes the spatial coordinates and extra prior intensity information of MR images with arbitrary undersampling scales for parallel imaging as input and then reconstructs corresponding high-quality MR images. The main contributions of this paper include:

- An implicit neural representation (INR) approach is proposed to represent fully-sampled MRI as a continuous function of spatial coordinates and prior pixel-specific features of undersampled MRI, which is parameterized by an MLP.
- We introduce a convolutional encoder network to produce pixel-specific features from the undersampled MRI as additional prior information input to the implicit function and thus recover pixel intensities without subject-specific constraint.
- The encoder is embedded by a reconstruction scale for generating uniform scale-independent features, which enables the implicit function to recover MRI with arbitrary undersampled scales for parallel imaging.
- Experimental results showed that compared with other parallel MRI reconstruction methods, our method obtained improved performance and generated images with superior quality.

2. METHODOLOGY

2.1. Problem Formulation

For an MRI system, the undersampled k-space signal y can be expressed as:

$$\mathbf{y} = \mathbf{A}I + \mathbf{n} \quad (1)$$

where I represents the image to be reconstructed and \mathbf{n} is the measurement noise. $\mathbf{A} = \mathbf{M}\mathbf{F}$ denotes degradation operator, where \mathbf{M} is a sampling mask and \mathbf{F} denotes the Fourier transform. In previous MRI reconstruction studies, the image I is restored by minimizing the following objective function:

$$\operatorname{argmin}_I \frac{1}{2} \|\mathbf{y} - \mathbf{A}I\|^2 \quad (2)$$

In INR, the MRI intensities I is regarded as a continuous coordinated-based implicit function, i.e., $f_\theta(\mathbf{x})$, where θ indicates the parameters of this function and $\mathbf{x} = (x, y)$ denotes

2D pixel coordinates, which are normalized to the range of $[-1, 1]$. Let I_θ be the discretized image matrix after uniform sampling from f_θ at the pixel locations. In this case, the reconstruction objective is rewritten as:

$$\operatorname{argmin}_\theta \frac{1}{2} \|\mathbf{y} - \mathbf{A}I_\theta\|^2 \quad (3)$$

Based on implicit neural representation (INR), f_θ is built as a multilayer perceptron (MLP). Thus, this reconstruction problem is transformed into training a network to optimize function (3).

2.2. Arbitrary Scale Reconstruction

To better learn the high-frequency feature, we adopt a positional encoding method from [16] to map the coordinates $\mathbf{x} \in \mathbb{R}^2$ to a higher dimension space \mathbb{R}^{2L} using an encoding function γ before passing coordinates to MLP:

$$\gamma(\mathbf{x}) = [\cos(2\pi B\mathbf{x}), \sin(2\pi B\mathbf{x})]^T \quad (4)$$

where B represents the encoding coefficients. Following [16], all entries of matrix B are sampled from Gaussian distribution $\mathcal{N}(\mathbf{0}, \sigma^2)$, where σ is a tunable hyperparameter. In this work, σ is set to 1.

It is impractical to train a specific function f_θ for each undersampled image. Instead, we need a generic one. Towards this end, the prior intensity information of the undersampled image is used as an extra input of f_θ , due to the lack of specificity of coordinates. Here, we induce a convolutional encoder network to compress the local pixel intensity of the input image into a pixel-specific feature map $V \in \mathbb{R}^{h \times w \times d}$. Thus, each feature vector in the feature map denoted by $v_{\mathbf{x}} \in \mathbb{R}^d$ contains the local semantic information of MR image at the coordinate \mathbf{x} , which helps MLP recover the specific pixel intensity.

It is worth noting that the undersampled scale of each MRI is not limited to a specific value in this recovery process, which means that the implicit function f_θ only learns the mapping from coordinates and feature vectors to pixel intensities. Thus, arbitrary scale reconstruction of MRI can theoretically be achieved. To have the ability to discriminate different reconstruction scales and generate a uniform scale-independent feature map, we embed the scale into the encoder:

$$v_{\mathbf{x}}^s = \text{Encoder}(I_u^s, s)(\mathbf{x}) \quad (5)$$

where s is the reconstruction scale, I_u^s is the undersampled MR image with the reconstruction scale s , and $v_{\mathbf{x}}^s$ denotes the prior feature vector of image I_u^s at the coordinate \mathbf{x} .

Finally, the implicit pixel function is:

$$I = f_\theta(\gamma(\mathbf{x}), v_{\mathbf{x}}^s) \quad (6)$$

f_θ and scale-embedded encoder are trained at the same time, and once the learning is complete, the MRI with arbitrary undersampled scale can be reconstructed in a short time.

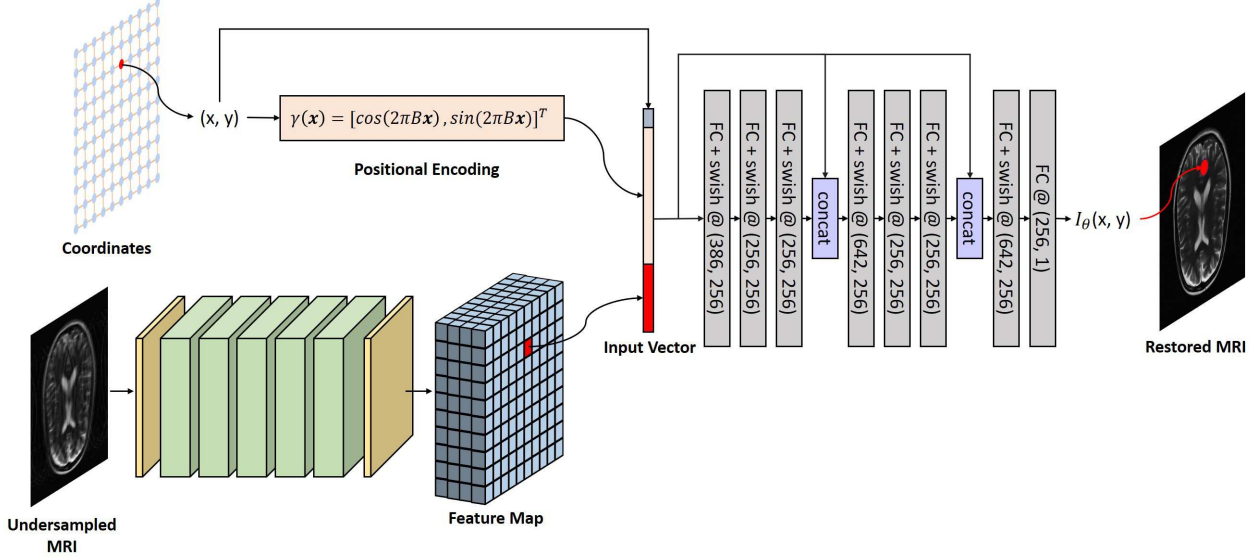


Fig. 1. The workflow of the proposed model. The undersampled image is first converted into a feature map through a scale-embedded encoder while the 2D pixel coordinates in the MRI grid are mapped into higher-dimension vectors. The feature vectors and the coordinates vectors are concatenated at each coordinate and fed into MLP to recover pixel intensities at each corresponding coordinate.

Considering that all the operations mentioned above are conducted in the image domain, we modify the reconstruction objective for convenient training of all networks:

$$\operatorname{argmin}_{\theta} \frac{1}{2} \|I^* - I_{\theta}\|^2 \quad (7)$$

where I^* denotes the fully-sampled MR image.

2.3. Overall Framework

The overall framework of our method is illustrated in Fig. 1. We first convert the undersampled image into a feature map through a convolutional encoder network with reconstruction scale embedding. In the meantime, the 2D pixel coordinates (x, y) in the MR image grid are mapped into higher-dimension vectors. The feature vectors and the coordinates vectors are concatenated at each coordinate and fed into MLP to recover pixel intensities at each corresponding coordinate. During training, the encoder and MLP are simultaneously optimized by minimizing the L1 loss between I^* and I_{θ} .

Specifically, the convolutional encoder network contains 5 scale-embedded residual blocks, all convolutional layers have 5x5 sized kernels for a large receptive field and 64 feature channels. We apply the group normalization [17] and use the swish [18] as our activation function. The positional encoding dimension $2L$ is set to 256 while the dimension d of feature vectors is 128. For MLP, the network has eight fully connected layers. All layers but the last are followed by a swish activation. Besides, we include three skip connections that concatenate the input of the network to the 4th and 7th

layers, respectively. Except that there are $2L+d$, $2L+d+256$, $2L+d+256$ neurons in the 1st, 4th, 7th layers, other have all 256 neurons.

3. EXPERIMENTS AND RESULTS

3.1. Implementation Details

All our experiments were implemented on a workstation with 64GB RAM and two NVIDIA GeForce RTX 2080 Ti graphics cards. Pytorch 1.8.1 was used as the back end. We trained our model for 100000 iterations using the ADAM optimizer with $\beta_1 = 0.9, \beta_2 = 0.99$, and set the batch size to 2. The initial learning rate was set to 0.001 and dropped by half in every 10000 iterations.

3.2. Dataset Description

Two types of MRI selected from the fastMRI dataset [19] were used in this study, which was collected at NYU Langone Health on Siemens scanners. One is fully sampled 15-channel knee k-space data, which was acquired using the 2D turbo spin-echo sequence without fat suppression. Another is fully-sampled T2 weighted 16-channel brain k-space data with 3T field strength. The oversampled region of raw data has been removed in our case. All selected datasets were uniformly undersampled with different reconstruction scales and 8% of the central region was reserved as auto-calibration signal (ACS) lines.

3.3. Experimental Results

In our experiments, we compared the proposed method with the GRAPPA [3], RAKI [20] and residual RAKI (rRAKI) [21] on two datasets with reconstruction scales=4, 5, and 6. Table 1 shows the quantitative evaluation results. We observe that the proposed method is significantly superior to all comparison methods, especially on the knee dataset, and achieves the best SSIM and the best or second-best PSNR in all experiments.

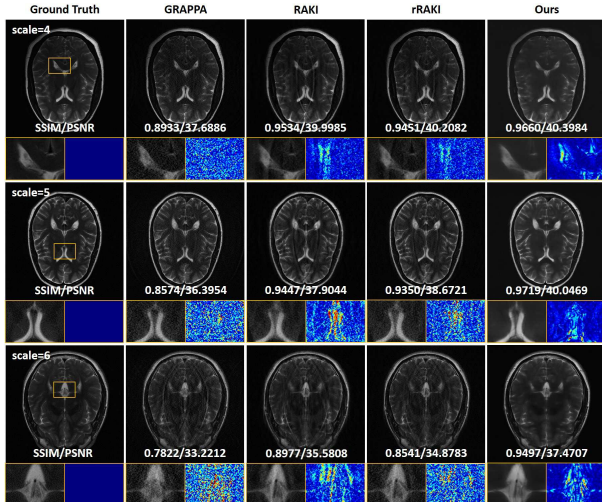


Fig. 2. Comparison of the qualitative performance of the proposed method and GRAPPA, RAKI, and rRAKI on the brain dataset.

Fig.2 visualizes the reconstruction effects of different methods on the three undersampled scales of the brain dataset. We can observe that these GRAPPA-reconstructed MR images are heavily noisy and suffer from obvious artifacts at higher reconstruction scales. In contrast, RAKI’s results have low noise levels and significantly improved SSIM and PSNR, however, artifacts remain a serious unresolved problem. The performance of rRAKI, including the quality of reconstructed images and evaluation metrics, is between GRAPPA and RAKI. The reconstruction effect of the three methods decreases sharply with the increase of the undersampled scale. On the contrary, the proposed method is more robust, which produces similar image quality at different undersampled scales without noise and obvious artifacts, and outperforms the compared methods.

The reconstruction results of different methods conducted on the knee dataset are shown in Fig.3. Similar to the experimental results on the brain dataset, GRAPPA, RAKI, and rRAKI still suffer from artifacts and noise. Furthermore, the images reconstructed by RAKI and rRAKI are more blurry with the boundaries between different tissues over-smoothed. Contrarily, the proposed method successfully reduces noise and artifacts that are apparent in the results of

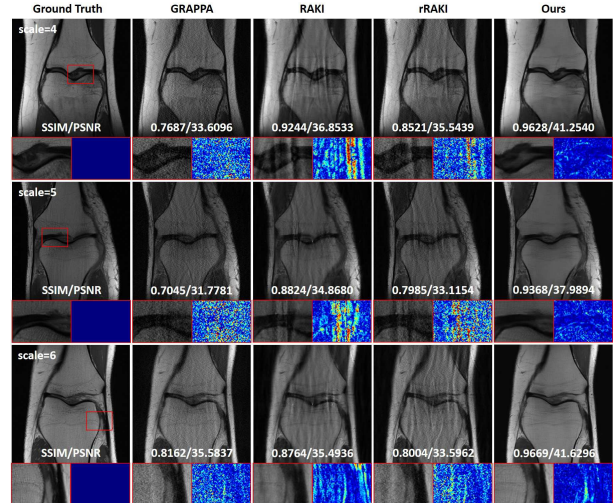


Fig. 3. Comparison of the qualitative performance of the proposed method and GRAPPA, RAKI, and rRAKI on the knee dataset.

the compared methods, as illustrated by the zoomed-in images in Fig.3, and restores images with both high definition detail and improved image contrast.

4. CONCLUSION

In this paper, we proposed an INR-based MRI reconstruction framework. Instead of learning the mapping from undersampled to fully-sampled MRI under a fixed reconstruction scale directly, we propose to learn a continuous implicit neural pixel function, which takes the higher-dimensional coordinates vectors and the scale-independent pixel-specific features generated by a convolutional scale-embedded encoder network as input to recover pixel intensities at each corresponding coordinate, thereby restoring high-quality MRI. Once the training of all networks of the proposed method is complete, it does not restrict the application to a specific subject or undersampled scale for MRI reconstruction. Our experimental results conducted on three different reconstruction scales show that the proposed method generates higher evaluation metrics and visual quality compared with some baseline models, making it potential for further accelerating MRI data acquisition.

5. LIMITATION

Despite the superior quality of MRI reconstruction, we acknowledge some limitations with our method. Firstly, due to the limitations of computational resources and data amount, the experiments in this paper only proved that our model can reconstruct MRI with three different undersampled scales. As for more or even arbitrary scales MRI reconstruction, larger

Table 1. Quantitative comparison with other reconstruction methods on the fastMRI dataset.

	Brain			Knee		
	$s = 4$	$s = 5$	$s = 6$	$s = 4$	$s = 5$	$s = 6$
GRAPPA [3]	0.8876/36.8103	0.8443/35.5809	0.7921/33.1173	0.7513/32.7750	0.6854/31.4585	0.7930/34.2945
RAKI [20]	0.9501/ 39.4045	0.9415/38.1688	0.8942/35.0135	0.9169/36.7898	0.8782/34.7770	0.8642/34.3090
rRAKI [21]	0.9317/38.9997	0.9222/38.0567	0.8450/33.9112	0.8440/35.2438	0.7769/32.6516	0.7739/32.3304
Ours	0.9543/37.7673	0.9624/39.1054	0.9461/36.8490	0.9480/39.4207	0.9406/38.8031	0.9532/39.8919

networks and more MRI data with more scales are theoretically required for training, which requires more research time, and the performance needs to be further verified in this case. Besides, we trained the proposed method in a supervised manner and depend heavily on fully-sampled and undersampled image pairs, impractical to obtain in the real-world clinical environment [22, 23], limiting the application. Therefore, an unsupervised version of the proposed method remains to be investigated.

6. REFERENCES

- [1] Michael Lustig, David Donoho, and John M Pauly, “Sparse MRI: The application of compressed sensing for rapid mr imaging,” *Magnetic Resonance in Medicine: An Official Journal of the International Society for Magnetic Resonance in Medicine*, vol. 58, no. 6, pp. 1182–1195, 2007.
- [2] Klaas P Pruessmann, Markus Weiger, Markus B Scheidegger, and Peter Boesiger, “SENSE: Sensitivity encoding for fast mri,” *Magnetic Resonance in Medicine: An Official Journal of the International Society for Magnetic Resonance in Medicine*, vol. 42, no. 5, pp. 952–962, 1999.
- [3] Mark A Griswold, Peter M Jakob, Robin M Heidemann, Mathias Nittka, Vladimir Jellus, Jianmin Wang, Berthold Kiefer, and Axel Haase, “Generalized autocalibrating partially parallel acquisitions (GRAPPA),” *Magnetic Resonance in Medicine: An Official Journal of the International Society for Magnetic Resonance in Medicine*, vol. 47, no. 6, pp. 1202–1210, 2002.
- [4] Gushan Zeng, Yi Guo, Jiaying Zhan, Zi Wang, Zongying Lai, Xiaofeng Du, Xiaobo Qu, and Di Guo, “A review on deep learning mri reconstruction without fully sampled k-space,” *BMC Medical Imaging*, vol. 21, no. 1, pp. 195, 2021.
- [5] Shanshan Wang, Zhenghang Su, Leslie Ying, Xi Peng, Shun Zhu, Feng Liang, Dagan Feng, and Dong Liang, “Accelerating magnetic resonance imaging via deep learning,” in *2016 IEEE 13th international symposium on biomedical imaging (ISBI)*. IEEE, 2016, pp. 514–517.
- [6] Mehmet Akçakaya, Steen Moeller, Sebastian Weingärtner, and Kâmil Uğurbil, “Scan-specific robust artificial-neural-networks for k-space interpolation (RAKI) reconstruction: Database-free deep learning for fast imaging,” *Magnetic Resonance in Medicine*, vol. 81, no. 1, pp. 439–453, 2019.
- [7] Hemant K Aggarwal, Merry P Mani, and Mathews Jacob, “MoDL: Model-based deep learning architecture for inverse problems,” *IEEE transactions on medical imaging*, vol. 38, no. 2, pp. 394–405, 2018.
- [8] Jian Sun, Huibin Li, Zongben Xu, et al., “Deep admm-net for compressive sensing mri,” *Advances in neural information processing systems*, vol. 29, 2016.
- [9] Zhiqin Chen and Hao Zhang, “Learning implicit fields for generative shape modeling,” in *Proceedings of the IEEE/CVF Conference on Computer Vision and Pattern Recognition*, 2019, pp. 5939–5948.
- [10] Ben Mildenhall, Pratul P Srinivasan, Matthew Tancik, Jonathan T Barron, Ravi Ramamoorthi, and Ren Ng, “Nerf: Representing scenes as neural radiance fields for view synthesis,” *Communications of the ACM*, vol. 65, no. 1, pp. 99–106, 2021.
- [11] Qing Wu, Yuwei Li, Lan Xu, Ruiming Feng, Hongjiang Wei, Qing Yang, Boliang Yu, Xiaozhao Liu, Jingyi Yu, and Yuyao Zhang, “IREM: High-resolution magnetic resonance image reconstruction via implicit neural representation,” in *Medical Image Computing and Computer Assisted Intervention–MICCAI 2021: 24th International Conference, Strasbourg, France, September 27–October 1, 2021, Proceedings, Part VI 24*. Springer, 2021, pp. 65–74.
- [12] Zixuan Chen, Jianhuang Lai, Lingxiao Yang, and Xiaohua Xie, “CuNeRF: Cube-based neural radiance field for zero-shot medical image arbitrary-scale super resolution,” *arXiv preprint arXiv:2303.16242*, 2023.
- [13] Liyue Shen, John Pauly, and Lei Xing, “NeRP: implicit neural representation learning with prior embedding for sparsely sampled image reconstruction,” *IEEE Transactions on Neural Networks and Learning Systems*, 2022.
- [14] Junshen Xu, Daniel Moyer, Borjan Gagoski, Juan Eugenio Iglesias, P Ellen Grant, Polina Golland, and Elfar Adalsteinsson, “NeSVoR: Implicit neural representation for slice-to-volume reconstruction in mri,” *IEEE Transactions on Medical Imaging*, 2023.
- [15] Ruimin Feng, Qing Wu, Yuyao Zhang, and Hongjiang Wei, “A scan-specific unsupervised method for parallel mri reconstruction via implicit neural representation,” in *2023 IEEE 20th International Symposium on Biomedical Imaging (ISBI)*. IEEE, 2023, pp. 1–5.
- [16] Matthew Tancik, Pratul Srinivasan, Ben Mildenhall, Sara Fridovich-Keil, Nithin Raghavan, Utkarsh Singhal, Ravi Ramamoorthi, Jonathan Barron, and Ren Ng, “Fourier features let networks learn high frequency functions in low dimensional domains,” *Advances in Neural Information Processing Systems*, vol. 33, pp. 7537–7547, 2020.
- [17] Yuxin Wu and Kaiming He, “Group normalization,” in *Proceedings of the European conference on computer vision (ECCV)*, 2018, pp. 3–19.
- [18] Prajit Ramachandran, Barret Zoph, and Quoc V Le, “Swish: A self-gated activation function,” *arXiv preprint arXiv:1710.05941*, vol. 7, no. 1, pp. 5, 2017.
- [19] Florian Knoll, Jure Zbontar, Anuroop Sriram, Matthew J. Muckley, Mary Bruno, Aaron Defazio, Marc Parente, Krzysztof J. Geras, Joe Katsnelson, Hersh Chandarana, Zizhao Zhang, Michal Drozdal, Adriana Romero, Michael Rabbat, Pascal Vincent, James Pinkerton, Duo Wang, Nafissa Yakubova, Erich Owens, C. Lawrence Zitnick, Michael P. Recht, Daniel K. Sodickson, and Yvonne W. Lui, “fastMRI: A publicly available raw k-space and dicom dataset of knee images for accelerated mr image reconstruction using machine learning,” *Radiology: Artificial Intelligence*, vol. 2, no. 1, pp. e190007, 2020, PMID: 32076662.
- [20] Mehmet Akçakaya, Steen Moeller, Sebastian Weingärtner, and Kâmil Uğurbil, “Scan-specific robust artificial-neural-networks for k-space interpolation (RAKI) reconstruction: Database-free deep learning for fast imaging,” *Magnetic resonance in medicine*, vol. 81, no. 1, pp. 439–453, 2019.
- [21] Chi Zhang, Steen Moeller, Omer Burak Demirel, Kâmil Uğurbil, and Mehmet Akçakaya, “Residual RAKI: A hybrid linear and non-linear approach for scan-specific k-space deep learning,” *NeuroImage*, vol. 256, pp. 119248, 2022.
- [22] Jianan Liu, Hao Li, Tao Huang, Euijoon Ahn, Adeel Razi, and Wei Xiang, “Unsupervised representation learning for 3d mri super resolution with degradation adaptation,” *arXiv preprint arXiv:2205.06891*, 2022.

- [23] Yusheng Zhou, Hao Li, Jianan Liu, Zhengmin Kong, Tao Huang, Euijoon Ah, and Zhihan Lv, “UNAEN: Unsupervised abnormality extraction network for mri motion artifact reduction,” *arXiv preprint arXiv:2301.01732*, 2023.